RESEARCH HIGHLIGHT

Cofactor-assisted dicing: insights from structural snapshots

Jiamu Du[1]✉ and Dinshaw J. Patel[2]✉

Cell Research (2022) 32:965–966; https://doi.org/10.1038/s41422-022-00716-9

Two recent cryo-EM publications in *Nature* by Su et al. and Yamaguchi et al. have captured snapshots of structures of *Drosophila* Dicer-2 bound to target dsRNA in the presence of protein cofactors Loquacious-PD or R2D2 along the small RNA biogenesis pathway, thereby highlighting the stepwise molecular mechanism underlying dicing-mediated precise small RNA production.

In eukaryotic cells, small RNAs (sRNAs) ranging in size from ~20 to 30 nucleotides (nt) are critical players in the RNA-mediated gene silencing pathway, playing key functional roles in gene regulation, development, DNA methylation and viral defense. Notably, dsRNA-derived small interfering RNAs (siRNAs) and endogenous hairpin RNA-derived microRNAs (miRNAs) both require the RNase III family endonuclease Dicer for their length-dependent and termini-specific biogenesis.[1] The Dicer nuclease plays a central role throughout all steps of the sRNA biogenesis pathway, including substrate RNA selection and loading, positioning of RNA within the active site, length-dependent dicing and release of the sRNA product to downstream Argonaute (Ago) effector proteins, through involvement of a set of conformational transitions in both its protein and RNA components.

Since its discovery, the molecular mechanism underlying Dicer's function has posed a central challenge in the sRNA field.[2] The initial crystal structure of minimalist (lacks a helicase domain) *Giardia intestinalis* Dicer in the apo state defined the alignment of protein subunits, which in turn allowed a biochemically validated model for positioning of dsRNA on Dicer, whereby RNA 3′-overhang recognition by the PAZ domain precisely positioned the dsRNA for length-dependent 2-base pair (bp) staggered cleavage by the composite pockets formed by the pair of RNase III domains.[3] This proposed 3′-counting rule was next updated by an additional 5′-counting rule where the cleavage site was measured primarily from the 5′-phosphate in the *Drosophila* system.[4]

To gain a structure-based understanding of the alignment and intermolecular contacts between Dicer and dsRNA, cryo-EM studies have been undertaken on both the human[5,6] and *Drosophila*[7] Dicer–dsRNA complexes, thereby providing insights into the pre-dicing conformation of the complex. These studies were followed by cryo-EM studies of plant Dicer DCL3 bound to pre-siRNA[8] and plant Dicer DCL1 bound to pri- and pre-miRNAs[9] in the active dicing-competent conformation that revealed additional insights into substrate selectivity and principles underlying RNA length measurement.

In *Drosophila*, Dicer-1 (Dcr-1) and Dicer-2 (Dcr-2) mediate miRNA and siRNA biogenesis pathways, respectively, with the assistance of dsRNA-binding domain (dsRBD) proteins Loquacious-PD (Loqs-PD), involved during conversion of dsRNAs into siRNAs, and R2D2, involved in loading of siRNAs into Ago2. *Drosophila* Dcr-2 is composed of N-terminal ATP-dependent helicase and DUF283 domains involved in dsRNA translocation, a central segment composed of a platform-PAZ-connector helix cassette involved in 5′- and 3′-end recognition, and a C-terminal pair of RNase III domains involved in 2-bp staggered cleavage of dsRNA (Fig. 1a, upper panel).

The paper by Su et al. reports on cryo-EM studies in the 3.1–4.6 Å range that captured distinct states of the complex of Dcr-2 bound to Loqs-PD (Fig. 1a, lower panel), 50-bp dsRNA, ATP and Mg^{2+} ions towards identification and characterization of individual steps, together with conformational transitions, during the full dicing reaction cycle.[10] Notably, the C-terminal tail of Loqs-PD is bound to the helicase domain of Dcr-2 in the complex. Thus, capitalizing on Dcr-2 mutants, the authors captured distinct conformations of the complex. Notably, upon dsRNA binding, the helicase and DUF283 domains transitioned from an extended to a closed conformation to specifically anchor the bound dsRNA through major and minor groove recognition, as well as generate ATP- and 5′-phosphate-binding pockets. In the next ATP hydrolysis-driven steps, 8-bp and 17-bp dsRNAs thread through the helicase domain towards the catalytic center of Dcr-2, reflecting states associated with early (Fig. 1b) and mid translocation steps, respectively. The overall conformation of the complex is quite rigid during the translocation steps, while blocking dsRNA access to the RNase active center. In addition, the dsRBD domain of Dcr-2 binds to the dsRNA, in the process bending and pushing the dsRNA towards the PAZ domain. Notably, ATP hydrolysis provides sufficient energy to pump the dsRNA through the helicase domain into the PAZ-platform cassette, in the process breaking the DUF283–RNaseIIIb interaction to achieve the fully active dicing conformation (Fig. 1c). The cleaved siRNA is released in the post-dicing state during a process accompanied by a shift in the conformation of the Dcr-2 PAZ-platform module, such that the helicase domain together with the remaining bound dsRNA is restored to its early translocation state, ready to start the next dicing cycle.

Previous functional studies established that R2D2 (Fig. 1a, lower panel) was required for the transfer of siRNA from Dcr-2 to Ago2, while retaining a defined orientation, whereby the 5′-terminus of the less stable end of the siRNA duplex is selected for loading into Ago2.[11] To this end, Yamaguchi et al.[12] solved the structure of R2D2-bound Dcr-2 in the absence and presence (Fig. 1d) of *let-7* siRNA at 3.3 Å resolution. In addition to siRNA bound to the helicase domain, which mimics the initial dsRNA binding state, a second siRNA duplex was observed bound to R2D2 in the

[1]Department of Biology, School of Life Sciences, Southern University of Science and Technology, Shenzhen, Guangdong, China. [2]Structural Biology Program, Memorial Sloan-Kettering Cancer Center, New York, NY, USA. ✉email: dujm@sustech.edu.cn; pateld@mskcc.org

Published online: 1 September 2022

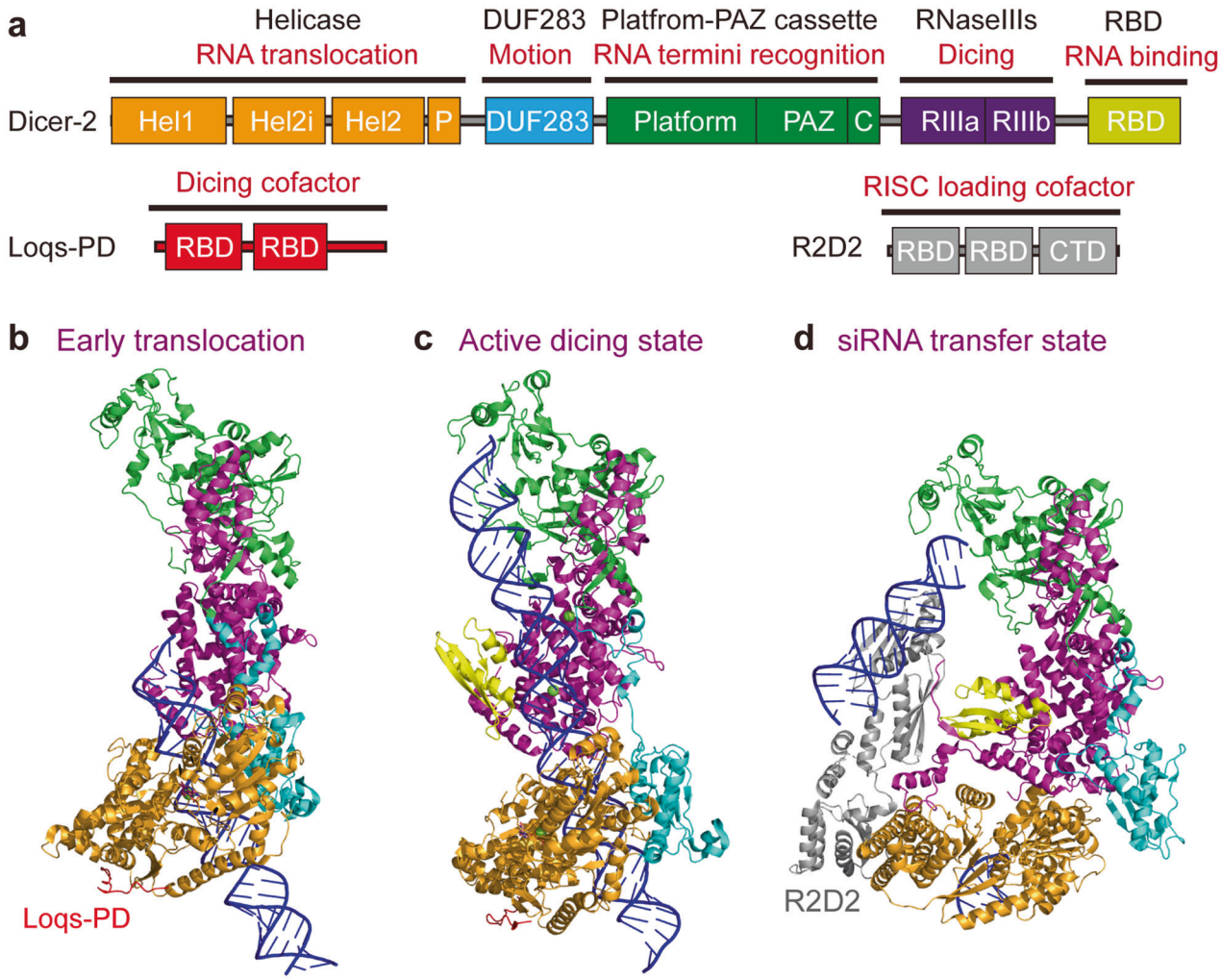

Fig. 1 Structural snapshots of dsRNA processing by Dicer-2. a Domain architecture of Dicer-2 (upper panel), Loqs-PD and R2D2 (lower panel). The domain cassettes and their main functions during dicing are labeled, respectively. P, Pincer-like domain; C, Connector helix. **b**, **c** Structures of Dicer-2–Loqs-PD bound to dsDNA in the early translocation (**b**; PDB: 7W0C) and active dicing (**c**; PDB: 7W0E) states. **d** Structure of Dicer-2–R2D2 bound to siRNA (PDB: 7V6C) revealing its orientation selection mechanism for siRNA recognition.

complex. Dcr-2 binds R2D2 via its helicase domain and a central linker segment, with RBD1 of R2D2 becoming ordered upon siRNA complex formation. Notably, R2D2 specifically recognized the stable end of the siRNA duplex in the complex, thereby exposing its unstable end to solvent and positioning it for capture by Ago2. These results provide a structural basis for sensing of the siRNA thermodynamic asymmetry and the mechanistic basis for loading of siRNA in a defined orientation onto Ago2, thereby identifying which strand of siRNA duplex is captured as the guide strand by Ago2 for target silencing. In addition, R2D2 also extensively interacted with the perfectly matched middle segment of siRNA, thereby preventing binding of central-mismatch-containing miRNAs, in the process serving as a siRNA/miRNA filter.

The papers by Su et al.[10] and Yamaguchi et al.[12] break new ground by definitively demonstrating the power of structural biology cryo-EM approaches to capture structural snapshots with mechanistic implications along the small RNA biogenesis pathway. These studies in turn set the stage for future investigation of the later steps of the siRNA biogenesis pathway, especially elucidating the molecular principles underlying loading of siRNA from Dcr-2–R2D2 onto Ago2 aided by the Hsc70/Hsp90 chaperone machinery.

REFERENCES

1. Kim, V. N., Han, J. & Siomi, M. C. *Nat. Rev. Mol. Cell Biol.* **10**, 126–139 (2009).
2. Bernstein, E., Caudy, A. A., Hammond, S. M. & Hannon, G. J. *Nature* **409**, 363–366 (2001).
3. Macrae, I. J. et al. *Science* **311**, 195–198 (2006).
4. Park, J. E. et al. *Nature* **475**, 201–205 (2011).
5. Taylor, D. W. et al. *Nat. Struct. Mol. Biol.* **20**, 662–670 (2013).
6. Liu, Z. et al. *Cell* **173**, 1549–1550 (2018).
7. Sinha, N. K., Iwasa, J., Shen, P. S. & Bass, B. L. *Science* **359**, 329–334 (2018).
8. Wang, Q. et al. *Science* **374**, 1152–1157 (2021).
9. Wei, X. et al. *Nat. Plants* **7**, 1389–1396 (2021).
10. Su, S. et al. *Nature* **607**, 399–406 (2022).
11. Tomari, Y. et al. *Science* **306**, 1377–1380 (2004).
12. Yamaguchi, S. et al. *Nature* **607**, 393–398 (2022).

ADDITIONAL INFORMATION

Correspondence and requests for materials should be addressed to Jiamu Du or Dinshaw J. Patel.